ACS APPLIED MATERIALS & INTERFACES

Research Article

www.acsami.org

Radio-Frequency-Transparent, Electrically Conductive Graphene Nanoribbon Thin Films as Deicing Heating Layers

Vladimir Volman,*[,†,‡] Yu Zhu,[§,‡] Abdul-Rahman O. Raji,[§] Bostjan Genorio,[§] Wei Lu,[§] Changsheng Xiang,[§] Carter Kittrell,[⊥] and James M. Tour*[,§,⊥,∥]

[†]Lockheed Martin Corp., MS2, Mail Stop 137-101, 199 Borton Landing Road, Moorestown, New Jersey 08057-0927, United States
[§]Department of Chemistry, [⊥]Richard E. Smalley Institute for Nanoscale Science and Technology, and [∥]Department of Mechanical Engineering and Materials Science, Rice University, 6100 Main Street, Houston, Texas 77005, United States

Supporting Information

ABSTRACT: Deicing heating layers are frequently used in covers of large radio-frequency (RF) equipment, such as radar, to remove ice that could damage the structures or make them unstable. Typically, the deicers are made using a metal framework and inorganic insulator; commercial resistive heating materials are often nontransparent to RF waves. The preparation of a sub-skin-depth thin film, whose thickness is very small relative to the RF skin (or penetration) depth, is the key to minimizing the RF absorption. The skin depth of typical metals is on the order of a micrometer at the gigahertz frequency range. As a result, it is very difficult for conventional conductive materials (such as metals) to form large-area sub-skin-depth films. In this report, we disclose a new deicing heating layer composite made using graphene nanoribbons (GNRs). We demonstrate that the GNR film is thin enough to permit RF transmission. This metal-free, ultralight, robust, and scalable graphene-based RF-transparent conductive coating could significantly reduce the size and cost of deicing coatings for RF equipment covers. This is important in many aviation and marine applications. This is a demonstration of the efficacy and applicability of GNRs to afford performances unattainable by conventional materials.

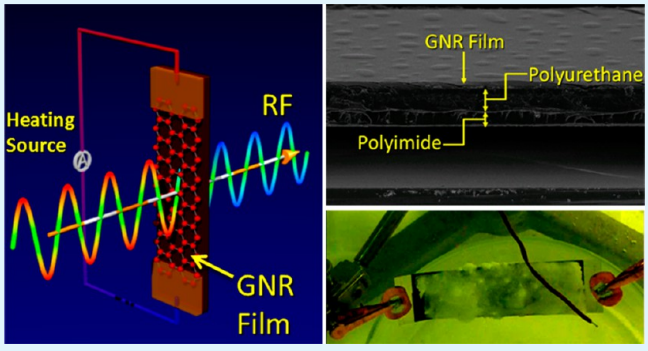

KEYWORDS: *graphene nanoribbon (GNR), radio-frequency (RF) transparent, electrically conductive film, carbon-based thin film, deicing, radome, radar, transmission loss, skin effect*

INTRODUCTION

Ice-elimination systems are very common in large radio-frequency (RF) structures. They can be classified as either passive antiicing films (preventing the accumulation of ice) or active deicing devices (removing ice after accumulation). A typical application of an icing protection system is in radomes. Radomes are protecting shells or covers for radar instruments in aviation and marine environments. The radomes are subject to hostile environments, such as high winds containing sand, rain, hailstones, and saltwater, over wide temperature variations. Explosive pressure blasts can also take place nearby the radomes. Thus, radome deicing conductive films must be extremely tough with good adhesiveness to the heated surface. In addition, these deicing structures must not compromise the reliability of the original RF system, which, in the case of radome applications, means that the deicing film must be predominately transparent to RF radiation at any polarization with minimal impact on the antenna scan performance. It is desirable that this film be lightweight and low-cost, with physical characteristics that allow it to cover large curved surface areas. Currently, most radome systems are constructed using a metal wire framework with supporting ceramic materials.[1−3] The metal wire framework serves as the conductive layer, and the ceramic materials are the heat-transfer medium. Because of the strong RF absorbance of metals, they need to be installed far from the RF source to achieve minimal RF attenuation. Consequently, current radomes are large, heavy, and costly, complicating their use on aircraft and ships.

The RF signals propagating through a material can be attenuated by absorption, reflection, or scattering.[4] Randomly dispersed multilayer graphene nanoribbons (GNRs) form isotropic or very close to isotropic conductive films. Each multilayer GNR component of the film is made of several crystallographically stacked narrow graphene monolayers that are 0.3 nm thick.[5−9] Because 1 nm = 10^{-6} mm, a film of 100 nm thickness is a tiny fraction of wavelength even for RF signals up to 300 GHz (1 mm wavelength). We can evaluate the

Received: September 25, 2013
Accepted: December 11, 2013
Published: December 11, 2013

 © 2013 American Chemical Society

propagation through such films using the classical skin effect concept[10] where the electrical field strength E (V/m) in the conductive layer decreases exponentially from its value at the surface, as in eq 1.

$$E \sim E_0 e^{-d/\Delta} \quad (1)$$

where d is the film thickness in meters and Δ is the distance at which incident E (i.e., E_0) diminishes to 1/e or ~37% of its original value (a detailed discussion of eq 1 is included in the Supporting Information). On the basis of this equation, the electrical field strength can be very small with an ultrathin conductive film (where $d \ll \Delta$). Because the GNR film is ultrathin, the electrical field variation is small and the electromagnetic waves reflected from the front and back surfaces of the film cancel each other because they are practically equal in magnitude and opposite in phase. Thus, we can expect a very low mismatch loss that is nearly insensitive to frequency. Then according to eq 2, the film full transmission loss L in decibels is defined by the frequency, the physical thickness of the film, and the conductivity of the film.

$$L = -126d\sqrt{f\sigma} \quad (2)$$

Here we disclose a new radome deicing coating based on an ultrathin conductive GNR film. A high-throughput spray-coating technique was developed to prepare GNR films that can function as the conductive layer for deicing coatings of large RF equipment such as bridge antenna towers and radome systems. In the new deicing system, the ultrathin GNR layer is used to conduct direct current (dc) or alternating current. The resistance of the GNR film is adjustable and is enough to generate sufficient heat for deicing the protected surface at voltages that are commonly used aboard ships and aircraft. The conductive GNR film is demonstrated to be thin enough to be transparent to RF signals. We have further demonstrated that ice formation on the protected surface can be prevented while the antenna array is operational.

EXPERIMENTAL METHODS

GNR Film Preparation. GNRs were synthesized based on previous reports.[11,12] GNRs were suspended in *o*-dichlorobenzene (ODCB) at a concentration of 1 mg/mL and bath-sonicated (12 W; model 08849-00, Cole-Parmer) immediately before use. The polyimide film (McMaster, 25 μm thickness) was cleaned with acetone and deionized water and dried. Polyurethane (clear-coat Dupli-Color auto paint, O'Reilly Auto Parts) was spray-coated on the polyimide substrate and dried at room temperature for 24 h. The polyurethane-coated polyimide substrate was placed atop a hot plate at 220 °C, and the GNR solution was spray-coated on the substrate using an Iwata airbrush connected to compressed nitrogen. The composite film was removed from the hot plate immediately after the spraying.

Waveguide Test and Simulation. A waveguide kit (WR-284) was first calibrated between 2.1 and 4 GHz. The sample was then mounted into the waveguide, and S_{11} and S_{21} were measured in series. The transmission coefficient in decibels is 10log (transmitted power/incident power). The transmission loss in decibels is -10log (transmitted power/incident power) or -transmission coefficient. The waveguide simulation was carried out by using Ansoft's high-frequency structure simulator (HFSS) 14.0.

Characterization. Scanning electron microscopy (SEM) images were taken using a JEOL 6500 scanning electron microscope and a FEI Quanta 400 field-emission gun scanning electron microscope. Transmission electron microsopy (TEM) images were taken using a 200 kV JEM 2100F microscope.

RESULTS AND DISCUSSION

Materials and Ultrathin GNR Film Preparation. The high-aspect-ratio, nonoxidized GNRs were synthesized by splitting multiwalled carbon nanotubes (MWCNTs) with potassium vapor or a sodium–potassium alloy.[11−13] The raw materials, MWCNTs, are much less expensive than single-walled carbon nanotubes. Over 500 tons/year of MWCNTs are produced. In one chemical step, MWCNTs are converted to GNRs, and the process is scalable. The produced GNRs (the TEM images of single GNRs used in this work are shown in Figure S1 in the Supporting Information) are free of oxidation and relatively conductive. In addition, they are solution-processable and compatible with many thin-film formation techniques such as spray, spin, or blade coating. Compared to graphene oxide, the GNRs are more promising materials for thin conductive film coatings because they need no annealing to achieve the high-conductivity state. The single GNRs exhibit conductivities over 60000 S/m.[11,12] The electrical conduction mechanism through the GNRs is the same as that through bulk graphite, as we have described in our previous work,[11,12] where detailed electrical measurements of the GNRs were performed. A significant difference between GNRs and bulk graphite is that it is much easier to attain an electrically percolative network with GNRs because of their high aspect ratio, thus facilitating the fabrication of conductive thin films. In comparison to other carbon materials, conventional carbon black has much lower conductivity compared to the GNRs. As a result, it requires much higher voltage to deliver the same amount of heat for the same size sample. It is thus not practical to use carbon black for resistive heating on equipment such as radomes. Although MWCNTs have conductivity similar to that of GNRs, the films produced from them would be thicker and would not meet the ultrathin film requirement for RF transparency because of their tubular structure. Functionalizing the sidewalls of nanotubes for dispersion in a solvent would make them less conductive compared to the GNRs, where only the edges are functionalized for enhanced dispersion. We have developed GNR-based thin films that were produced using large-area coating techniques such as spray coating.[14,15] Our previous work demonstrated that GNRs can be dispersed in ODCB at concentrations up to ~1 mg/mL.[11] Here, the GNRs were synthesized based on the reported work and dispersed in ODCB, and the dispersion was used in a high-throughput spray-coating procedure for preparing thin GNR films on polymer substrates.

GNR films with various thicknesses and sheet resistances were prepared (see the Experimental Methods for details). Polyimide was used as the substrate in this work because it is resistant to the ODCB solvent and stable to >200 °C. In the initial test, it was found that the GNR films did not adhere well to the polyimide substrate. Thus, commercially available clear-coat Dupli-Color automotive paint (pigment- and dye-free polyurethane, which adheres well to the substrate) was used as an adhesive layer in which the GNRs could be embedded. The polyurethane (~30 nm thick) was spray-coated on the polyimide and permitted to dry. Polyurethane was found to be a robust protective coating that works well in our experiments. The polyimide–polyurethane film was then placed on a 200 °C hot plate in a fume hood. The ODCB suspension of the GNRs was then spray-coated atop the polyurethane, whereupon ODCB rapidly evaporated, leaving the GNRs well-embedded in the polyurethane adhesion layer.

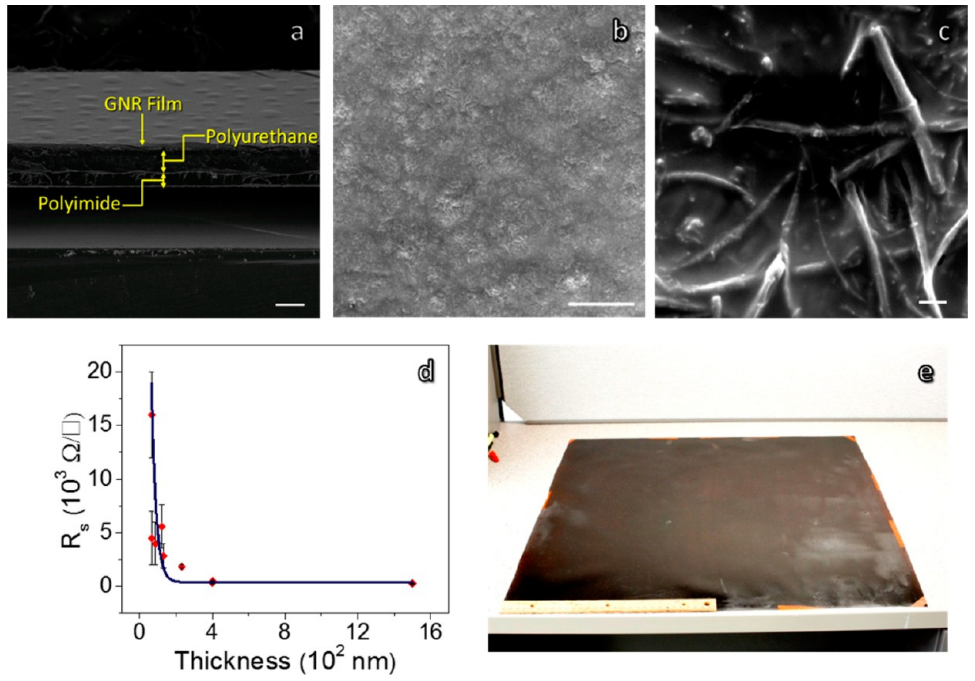

Figure 1. Characterization of ultrathin GNR films. (a) SEM cross-sectional image of the ultrathin GNR film. The bottom layer is the polyimide substrate (25 μm thick). The middle is the clear-coat Dulpi-Color automotive paint (pigment- and dye-free polyurethane). The upper layer is the GNR film, which is also embedded in the polyurethane layer. Scale bar = 100 μm. (b) Top view of the SEM image of the GNR film that shows GNRs embedded in the polyurethane. Scale bar = 100 μm. (c) High-resolution SEM image of the GNR film. The GNRs are entangled to form a conducting percolated network embedded in polyurethane. The center dark rectangular region was formed while focusing the instrument because of the charging effect of the polymer substrate. Scale bar = 1 μm. (d) Relationship of the GNR film thickness and sheet resistance. The sheet resistance was determined by the four-point probe method. (e) A 0.6 × 0.6 m^2 (2 × 2 ft^2) GNR film on polyimide. This sample was prepared in the laboratory using the spray-coating technique and a commercially available air brush. The large film was heated using three heating plates covered with a 1.3 cm (0.5 in) thick panel of aluminum. A 30.5 cm (1 ft) ruler is in the lower left.

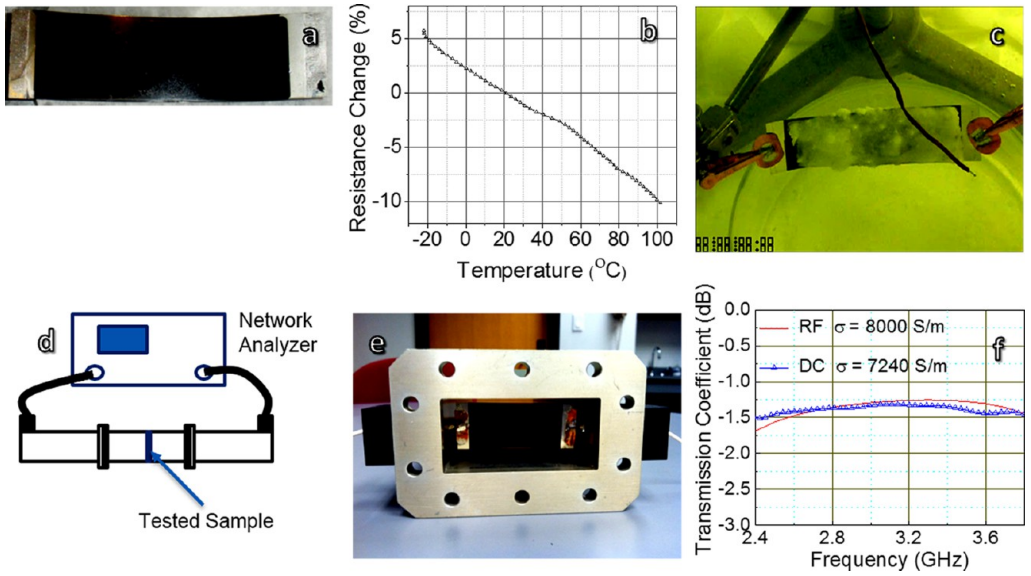

Figure 2. Deicing and transmittance tests. (a) Polyimide/polyurethane/GNR sample with platinum coated at the two ends. The size of the active GNR film (the center black region) is 25.4 × 76.2 mm^2. (b) GNR film resistance change over a temperature range. (c) Picture from the video of the deicing demonstration at −20 °C. The GNR film is connected to two flat copper clamps that are connected to the power source. The ice is preformed on the surface of the GNR film. The wire hanging above the GNR film is a thermocouple to monitor the environmental temperature, which is maintained at −20 °C within the experimental observation box. With the current passing through the film, the ice is melted in minutes (see the Supporting Information for the full video). (d) Block diagram of the RF test assembly. The sample is mounted between two waveguides, and the RF wave was generated and analyzed by a network analyzer. The sample can be rotated in order to acquire the transmission coefficient at different angles. (e) WR-284 waveguide with the wired GNR film. (f) Transmission coefficient in decibels versus frequency for a GNR-coated polyimide film: comparison of HFSS simulated and experimental data. The red line is based on the HFSS simulation with a GNR film of 8 kS/m RF conductivity and 110 nm thickness. The blue line is the RF measurement of a 110-nm-thick GNR polyimide film with 7.24 kS/m dc conductivity.

dx.doi.org/10.1021/am404203y | ACS Appl. Mater. Interfaces 2014, 6, 298−304

Table 1. Properties of GNR Films on a Polyimide Substrate Used for dc and RF Measurements[a]

	R_s (kΩ/□)	R (kΩ)	dc conductivity (kS/m)	approximate GNR film thickness (nm)	sample size (width × length, mm)	V (V)	I (mA)	calculated energy delivered (W)
1	1.02	3.06	5.77	170	25.4 × 76.2	151.5	49.5	7.5
2	1.92	5.76	5.21	100	25.4 × 76.2	207.8	36.1	7.5
3	4.85	14.56	2.58	80	25.4 × 76.2	330.0	22.7	7.5
4	1.26	2.51	7.24	110	25.4 × 50.8			
5	4.97	9.94	2.68	75	25.4 × 50.8			

[a] R_s is the sheet resistance measured by a four-point probe. R is the dc resistance of the active GNR film. Rs values are lower than R values of films because they were measured for a smaller area. The GNR film thickness was estimated based on Figure 1d. The dc conductivity was calculated based on the resistance and the thickness. V and I are the applied voltage and current, during deicing, respectively. Films 4 and 5 are smaller because they needed to fit into a waveguide. This is the reason for the opposite trend between the sheet and dc resistance between samples 1 and 4 and samples 3 and 5.

Parts a–c of Figure 1 show the SEM images of ultrathin GNR films on flexible polyimide substrates. The GNRs were embedded throughout the adhesive polyurethane layer to form a network that is conductive through percolation. This composite film is very robust, and removal requires sandpaper treatment. The GNRs are not removable by touch or by pulling on the surface with adhesive tape. Through control of the spraying time or GNR solution concentrations, the thickness of the GNR films can be tuned to modulate the resistance of the films. The sheet resistance versus GNR film thickness was studied, and the results are shown in Figure 1d. Large samples, such as the GNR film panel measuring 0.6 × 0.6 m^2 (2 × 2 ft^2) in Figure 1e, were prepared in the laboratory.

Design of GNR Films for Radome Deicing Coatings. The dc conductivity was calculated through the measured resistance, as shown in eq 3:

$$\sigma = \frac{l}{AR} \tag{3}$$

where $A = wt$, in which A is the GNR layer cross-sectional area (nm^2), w is the GNR layer width (nm), t is GNR layer thickness (nm), l is the GNR layer length (nm), and R is the resistance (kΩ).

In order to melt ice on the surface, a heating power density of ∼0.386 W/cm^2 (2.5 W/in^2) is used because this is a common ship-board power-delivery quantity. As for the test, small samples (Figure S2 in the Supporting Information) were prepared. The two ends of the sample were sputter-coated with platinum as the electrodes, and the size of the active GNR film was 25.4 × 76.2 mm^2 (1 × 3 $in.^2$; Figure 2a and Table 1, entries 1–3). The parameters of the samples are presented in Table 1 (entries 1–3). The voltage and current required to deliver the power were calculated based on Ohm's law. The results show that the voltage and current are within the applicable range of a common ship or aircraft power supply.

For practical applications, it is important to know how the GNR film responds to temperature variations. The results of thermal tests are shown in Figure 2b. The experimental setup to determine the temperature-dependent resistance of GNR films is shown in Figure S3 in the Supporting Information. According to the data, the GNR film has a negative temperature coefficient, which affords a much narrower range of temperature dependence than that found in typical metals such as copper, aluminum, or silver. The variation of the resistance is −10% from 20 to 100 °C, significantly smaller than those for metals (typically +30% from 20 to 100 °C). The smaller resistance change to the temperature is very helpful for these applications. Thus, the GNR film delivers more reliable power from a stabilized voltage supply across any temperature range.

To demonstrate that the GNR film can meet the heat power requirements, the GNR film on polyimide shown in Figure 2a was put at a 45° angle with 5 g of ice that was grown atop the film. The ice had been grown by placing the polyimide/polyurethane/GNR film on a block of dry ice and spraying it with water from a mist bottle until the film accumulated 5 g of ice. A fan blowing over the dry ice provided a −20 °C atmosphere in an insulated box to simulate freezing conditions, as recorded by the thermocouple above the film sample (Figure 2c). The dc power supply was connected to film electrodes, as shown in Figure 2c. After 3 min, the ice was completely removed from the area around the center of the GNR film; it took another 2.5 min to melt the ice close to the electrodes (Figure S4 in the Supporting Information).

RF Conductivity Measurements. It well-known that the bulk conductors such as silver, gold, or copper have similar dc and RF (in the gigahertz frequency range) conductivities.[16] Prior published work concerning graphene RF conductance was focused on measurements of few-layered graphene, where the RF conductance of few-layered graphene slightly increases with the frequency; at 4 GHz, it is ∼1.5 times higher than the dc conductance.[17] Thus, classical skin-depth theory does not hold. However, the GNR films of ∼100 nm thickness that are made of electrically percolating, long GNRs are structurally distinct from a few-layered, continuous sheet of graphene. Therefore, it is necessary to explore the actual RF conductivity of the GNR thin film that is much thinner than the skin depth. It is also important to determine the correlation between the dc and RF conductivity to assess the applicability of normal classical skin-depth theory in order to verify the equations introduced earlier for this specific system.

In this work, an **S**-matrix measurement waveguide technique was used to experimentally determine the RF conductivity. A GNR film with 110 nm thickness was prepared and the dc conductivity was measured to be 7240 S/m (entry 4 in Table 1). The film was fitted in the perpendicular position within a rectangular waveguide and was measured using a Vector Network Analyzer (Figure 2d). Figure 2e shows the GNR film mounted within the S-band WR-284 rectangular waveguide (to fit the size of the waveguide, the sample size was decreased to 25.4 × 50.8 mm^2). Because the WR-284 waveguide cutoff frequency of the dominant mode is 2.08 GHz and the first high mode starts propagation at 4.16 GHz, all of the measurements were taken between 2.4 GHz (far enough from the dominant mode cutoff frequency to achieve low empty waveguide transmission loss) and 4 GHz (to be sure of a negligible level of high modes). The scattering parameters such as the

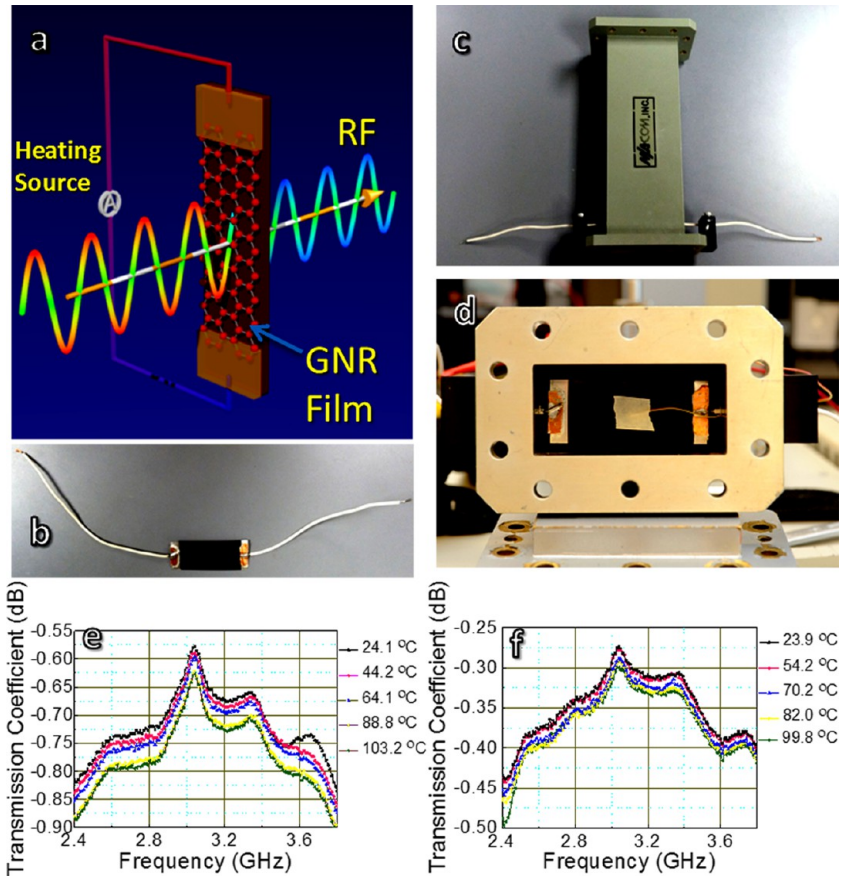

Figure 3. Real-time waveguide transmission test results. (a) Scheme of the real-time waveguide transmission test. The current passes through the GNR film during the RF measurement. This is to simulate the RF signal transmission when the deicing is progressing. (b) Wired GNR films. (c) Overview of the waveguide with the wired GNR film installed. (d) WR-284 waveguide with the wired GNR film. The thermal sensor is under the white tape patch covering the sensor, and it monitors the surface temperature of the GNR film. (e) Real-time waveguide transmission coefficient of the GNR film with a thickness of 110 nm (entry 4 in Table 1). (f) Real-time waveguide transmission coefficient of the GNR films with a thickness of 75 nm (entry 5 in Table 1). The legend on the right in parts e and f is the surface temperature of the GNR layer.

reflection (S_{11}) and transmission (S_{21}) of the waveguide section with and without GNR film samples were collected. Then the measured data (blue line in Figure 2f) were compared with the simulated transmission coefficient from Ansoft's HFSS to determine the RF conductivity. The details of the HFSS simulation are described in Figure S5 in the Supporting Information. The exact HFSS model of the same GNR film on a substrate was simulated with several RF conductivity values close to the dc conductivity value of the film. It was found that the best match between the measured and simulated data took place if the HFSS model of the GNR film had a RF conductivity of 8000 S/m (red line in Figure 2f). The ~9% difference between the dc and RF conductivities was expected and is predominantly related to a mismatch loss. The measured reflection coefficient from the GNR film alone, with no electrodes, is below −20 dB. The reflection of electromagnetic waves from the GNR layer can be calculated as the superposition of all electromagnetic waves reflected at the front and back boundaries between areas of different dielectric properties. Because of the extremely small GNR film thickness in comparison to the wavelength at S-band frequencies, most of these reflected waves cancel each other. Additional GNR films were tested, and the RF sheet resistance values are plotted with dc sheet resistance values in Figure S6 in the Supporting Information. In all cases, a very good correlation between the dc and RF conductivities was demonstrated. A good match between HFSS simulations based on normal classical skin-depth theory and the experimental waveguide tests shows that conventional conductive material concepts hold for the GNR films.

Real-Time Waveguide Transmission Test. The real-time waveguide transmission test scheme is shown in Figure 3a. The setup is shown in Figure 3b–d. A two-port network analyzer was calibrated without a GNR film inside the waveguide between 2.4 and 3.8 GHz, and it provides a measurement of the complex transmission and reflection coefficients S_{ij} of the **S** matrix in eq 4:

$$\mathbf{S} = \begin{bmatrix} S_{11} & S_{12} \\ S_{21} & S_{22} \end{bmatrix} \tag{4}$$

In Figure 3d, the two wide copper electrodes plated on the GNR layer are parallel to the vector of the electrical field in the waveguide, which formed an inductance diaphragm and served as a source of additional reflections. Therefore, an additional test was carried out to determine the reflection from the diaphragm only. The transmission coefficient of the GNR layer was calculated as the difference between the transmission coefficient of the GNR layer plus electrodes and the transmission coefficient of the electrodes only. The results of these measurements are shown in Figure 3e,f.

dx.doi.org/10.1021/am404203y | ACS Appl. Mater. Interfaces 2014, 6, 298–304

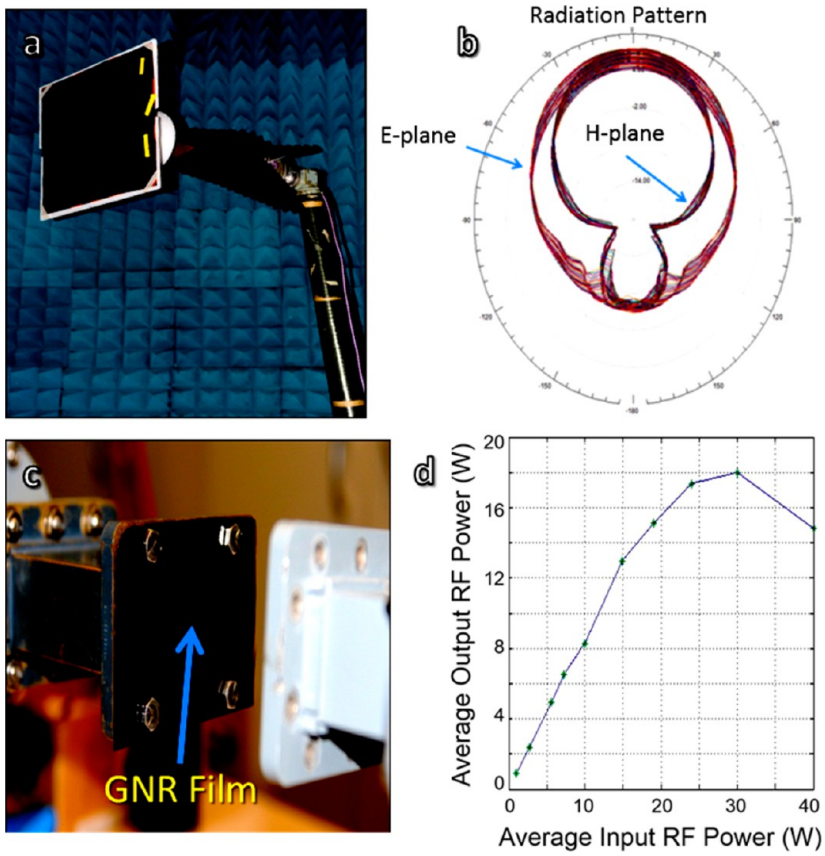

Figure 4. Antenna range test and high-power test results. (a) A 0.6 × 0.6 m^2 (2 × 2 ft^2) GNR film in front of an open waveguide for the antenna range test. (b) HFSS-simulated radiation pattern of an open waveguide with a GNR film in front. The angles are labeled in 30° clockwise increments from 0° at the top to 150°, −180° at the bottom, and from −150° to −30°. (c) GNR film window in a WR-284 waveguide for the high-power test. (d) Plot of the average output power versus input power. The linear region is up to 25 W in this specific case. The nonlinear behavior after 25 W is probably due to carbonization of the polymer substrate.

During the real-time waveguide transmission test, the voltage was applied to the GNR films to simulate the deicing working status. The RF transimission experiment was carried out simultaneously. As the current passes through the GNR films, the films become hot, and the surface temperature of the film was recorded by a flat thermocouple. The transmission coefficient decreases as the layer temperature increases (i.e., RF transmission decreases with temperature; Figure 3e,f). Thus, the RF transmission has the same negative temperature coefficient as the dc resistance. As expected, the GNR film behaves as a classical conductor with respect to the electromagnetic wave despite its negative temperature coefficient of resistance. Even though the loss slightly increases with temperature, it is still small because the material is much thinner than the skin depth. According to the results in Figure 3e,f, the transmission loss of a GNR film depends on the thickness and conductivity of the layer. For the GNR sample with a thickness of ∼110 nm, the transmission loss did not exceed 0.9 dB in the range of 2.4 to 3.8 GHz. The sample of 75 nm thickness exhibited a better loss of <0.5 dB. The testing results convincingly suggest that the GNR films can replace the conventional deicing heat circuits, thereby improving the radome performance.

Antenna Range Rest and High Power Test. Advanced modern radars are highly sophisticated systems with well-designed radomes that not only protect the enclosed radar antenna from harsh environments such as ice or freezing rain but also have a low impact on the electrical performance of the antenna. Therefore, we must be sure that the additional GNR deicing layer on top of the radome does not lead to antenna system degradation such as significant gain reduction, side-lobe increase, depolarization, antenna beam steering, and broadband performance. The objectives of the antenna range test described below were to verify the GNR film's high-RF transparency for any incident wave within the angular sector ±60° in wide-frequency bands.

A large 0.6 × 0.6 m^2 (2 × 2 ft^2) GNR film for an antenna range test was prepared on a flexible polyimide substrate (Figure 1e). Figure 4a shows the large GNR film that was affixed in front of an open WR-284 rectangular waveguide to check the impact of the film on this simple antenna gain, cross-polarization performance, and shape of its pattern diagram. Because the return loss of this film measured in the waveguide was below −20 dB, the main reduction in the peak gain was related to the transmission loss (Figure 4b). The transmission loss was in the range of 0.2−0.4 dB at a frequency band of 2.6−4.0 GHz for any polarization in the angular sector ±60°. No depolarization effect was detected. The testing results are in good agreement with the HFSS model based on classical skin-depth analysis, which is shown in Figure 4b.

The high-power tests were carried out in waveguide WR-284 with the GNR film located between two waveguide flanges, as shown in Figure 4c. The typical dependence of the average output power versus average input power is shown in Figure

dx.doi.org/10.1021/am404203y | ACS Appl. Mater. Interfaces 2014, 6, 298−304

4d. The linear characteristic behavior of input and output power is up to 25 W (power density of about 20 kW/m^2), which is quite good for most antenna applications. The nonlinear behavior was observed when the power was further increased (in the sample shown in Figure 4d, >25 W). One possible explanation, based on this test, is that the RF-transparent GNR film did absorb a small amount of RF energy that heated the polyurethane and polyimide substrates of the film, leading to a change of the film morphology or carbonization in the extreme case. However, it should be emphasized that the power density of ∼20 kW/m^2 already meets most antenna application specifications, and further improvement in the substrate materials could enhance the high-power test performance. We conjecture that there are local regions of thicker GNR film thickness because of puddling during spray coating of the GNRs onto the wavy polyimide film. New, more planar substrates are therefore being investigated to address this problem.

CONCLUSION

In this work, a robust GNR film was integrated onto a flexible polymer substrate, and its application as a radome deicer was evaluated. On the basis of the RF transmission test (from 2.4 to 3.8 GHz) and simulations, the transmission loss was ultralow and did not exceed 0.5 dB for any frequency below 3.8 GHz for a GNR film with a thickness of 75 nm and did not exceed 1 dB for a film with a thickness of 110 nm. The antenna range tests showed that the measured transmission loss was in the range of 0.2−0.4 dB for any polarization in the angular sector ±60°. No depolarization effect was detected. The deicing capability of the GNR films was evaluated at −20 °C, and the efficient removal of an ice coating under those cold conditions was demonstrated. To the best of our knowledge, there is no existing design of a deicing system that can provide such a RF-transparent performance combined with low-weight, low-cost materials. This underscores the efficacy of the GNR-based nanomaterial for a performance unattained by conventional materials.

ASSOCIATED CONTENT

Supporting Information

Detailed derivation of an electromagnetic field through a thin GNR film, high-resolution TEM images of GNRs, images of GNR films on polyurethane-coated polyimide substrates, experimental setup for measuring the resistance of the GNR film under different temperatures, description of the deicing video, details of the deicing test under −20 °C conditions, HFSS infinite GNR film model, and dc sheet resistance versus RF sheet resistance. This material is available free of charge via the Internet at http://pubs.acs.org.

AUTHOR INFORMATION

Corresponding Authors

*E-mail: vlad.vlad@verizon.net.
*E-mail: tour@rice.edu.

Author Contributions

‡These authors have contributed equally

Notes

The authors declare the following competing financial interest(s): Y.Z., V.V., and J.M.T. are coinventors on patent applications (US201220808A1 and WO2012100178A1) owned by Rice University and Lockheed Martin Corp. that disclose the use of RF-transparent GNR films for radome deicing circuits.

ACKNOWLEDGMENTS

The Lockheed Martin Corp. through the LANCER IV Program provided funding, fabrication, and testing support. The AFOSR (Grant FA9550-09-1-0581), the AFOSR MURI (Grant FA9550-12-1-0035), and the ONR MURI Graphene Program (No. 00006766, N00014-09-1-1066) provided funding for GNR development.

REFERENCES

(1) Harris, D. C. *Materials for Infrared Windows and Domes: Properties and Performance*; SPIE Press: Bellingham, WA, 1999; p 80.
(2) Walton, J. D. *Am. Ceram. Soc. Bull.* **1974**, *53*, 255−258.
(3) Kirby, K. W.; Jankiewicz, A.; Kupp, D.; Walls, C.; Janney, M. *Mater. Technol.* **2001**, *16*, 187−190.
(4) Ramo, S.; Whinnery, J. R.; Van Duzer, T. *Fields and Waves in Communications Electronics*; John Wiley & Sons: New York, 1994; pp 677−741.
(5) Novoselov, K. S.; Geim, A. K.; Morozov, S. V.; Jiang, D.; Zhang, Y.; Dubonos, S. V.; Grigorieva, I. V.; Firsov, A. A. *Science* **2004**, *306*, 666−669.
(6) Novoselov, K. S.; Geim, A. K.; Morozov, S. V.; Jiang, D.; Katsnelson, M. I.; Grigorieva, I. V.; Dubonos, S. V.; Firsov, A. A. *Nature* **2005**, *438*, 197−200.
(7) Geim, A. K. *Science* **2009**, *324*, 1530−1534.
(8) Li, X.; Cai, W.; An, J.; Kim, S.; Nah, J.; Yang, D.; Piner, R.; Velamakanni, A.; Jung, I.; Tutuc, E.; Banerjee, S. K.; Colombo, L.; Ruoff, R. S. *Science* **2009**, *324*, 1312−1314.
(9) Sun, Z.; Yan, Z.; Yao, J.; Beitler, E.; Zhu, Y.; Tour, J. M. *Nature* **2010**, *468*, 549−552.
(10) Jordan, E. *Electromagnetic Waves and Radiating Systems*; Prentice Hall: Englewood Cliffs, NJ, 1968; pp 129−130.
(11) Genorio, B.; Lu, W.; Dimiev, A. M.; Zhu, Y.; Raji, A.-R. O.; Novosel, B.; Alemany, L. B.; Tour, J. M. *ACS Nano* **2012**, *6*, 4231−4240.
(12) Kosynkin, D. V.; Lu, W.; Sinitskii, A.; Pera, G.; Sun, Z.; Tour, J. M. *ACS Nano* **2011**, *5*, 968−974.
(13) Lu, W.; Ruan, G.; Genorio, G.; Zhu, Y.; Novosel, B.; Peng, G.; Tour, J. M. *ACS Nano* **2013**, *7*, 2669−2675.
(14) Zhu, Y.; Lu, W.; Sun, Z.; Kosynkin, D. V.; Yao, J.; Tour, J. M. *Chem. Mater.* **2011**, *23*, 935−939.
(15) Xiang, C.; Lu, W.; Zhu, Y.; Sun, Z.; Yan, Z.; Hwang, C.-C.; Tour, J. M. *ACS Appl. Mater. Interfaces* **2012**, *4*, 131−136.
(16) Thorp, J. S. *Proc. Inst. Electr. Eng., Part 3* **1954**, *101*, 357−359.
(17) Rouhi, N.; Jain, D.; Capdevila, S.; Jofre, L.; Brown, E.; Burke, P. J. Broadband Conductivity of Graphene from DC to THz. In Nanowires/CNTs/Graphene: Properties of Graphene I. *Proceedings of the IEEE International Conference on Nanotechnology*, Portland, OR, Aug 15−18, 2011; IEEE: Piscataway, NJ, 2011; pp 1205−1207.